

**A DYNAMIC COUPLED THERMAL RESERVOIR
APPROACH TO ATMOSPHERIC ENERGY TRANSFER
PART III: THE SURFACE TEMPERATURE**

Roy Clark PhD

Ventura Photonics Monograph VPM 004.1

September 2019

Ventura Photonics
Thousand Oaks, CA

TABLE OF CONTENTS

Appendix: Detailed Model Description 2
 A1: The Surface Flux Balance 2
 A2: Land Surface Temperature Model 4
 A3: Ocean Surface Temperature Model 8



APPENDIX: DETAILED MODEL DESCRIPTION

A1: The Surface Flux Balance

The various flux terms illustrated above in Figure 1 will now be considered in more detail.

For a time interval Δt , the change in surface temperature ΔT is given by the basic surface flux balance equation [Clark, 2013a].

$$\Delta T = (\Delta Q_{\text{sunabs}} - \Delta Q_{\text{imet}} - \Delta Q_{\text{sens}} - \Delta Q_{\text{lat}} - \Delta Q_{\text{ssc}}) / C_s x \quad (\text{A1})$$

where C_s is the heat capacity of the surface layer, T is the surface layer temperature and x is the layer thickness, Q_{sunabs} is the absorbed solar flux, Q_{imet} is the net LWIR cooling flux, Q_{sens} is the sensible heat flux or dry air convection, Q_{lat} is the latent heat flux and Q_{ssc} is the subsurface heat transport. The time interval is typically 0.5 to 2 hours, based on short term meteorological station data averages. Long term climate change is determined by the overall trend in the short term data. This flux balance approach is common engineering practice. It is used for example in the evaluation of solar heating effects in overhead electrical power lines [IEEE, 1993].

The air-land and the air-ocean interfaces have rather different thermal properties and have to be treated separately. However, the important point that seems to have been overlooked is that all of the cooling terms in Eqn. A1 require a thermal gradient or temperature difference. For evaporation, the temperature difference is part of the humidity gradient. The Earth's climate is controlled by the Second Law of Thermodynamics, not the First. Conservation of energy is still required, but the thermal storage and time dependent thermal transfer properties of the thermal reservoirs must be explicitly included in any realistic description of the surface temperature.

The incident 'clear sky' solar flux may be determined using a polynomial expansion of the solar elevation angle θ_e [IEEE, 1993].

$$\Delta Q_{\text{sun}} = (A + B\theta_e + C\theta_e^2 + D\theta_e^3 \dots\dots\dots) \quad (\text{A2})$$

θ_e is calculated from the hour angle, h , the solar declination δ and the local latitude ϕ .

$$\sin\theta_e = \cosh\cos\delta\cos\phi + \sin\delta\sin\phi \quad (\text{A3})$$

The fraction of the solar flux absorbed at the land surface depends on the angle of incidence and the surface absorbance. Over the oceans, the water surface is almost transparent. Approximately half of the total solar flux is absorbed within the first meter of the ocean and the remainder is absorbed within the first 100 meters or less.

For the land surface, the absorbed solar flux is given by

$$Q_{\text{sunabs}} = A_{\text{surf}}(1-R_{\theta})Q_{\text{sun}}\text{Cos}\theta \quad (\text{A4})$$

where A_{surf} is the surface absorption and R_{θ} is the angle dependent surface reflection and $\text{Cos}\theta$ is the Lambert cosine term.

For the ocean-air interface, A_{surf} has to be modified to incorporate the depth dependence of the solar flux absorption:

$$Q_{N\text{sunabs}} = A_N x_N Q_{\text{sun}} \left[1 - \sum_1^{N-1} A_N x_N \right] \quad (\text{A5})$$

where A_N is the flux fraction absorbed in the Nth ocean layer with thickness x_N .

The solar flux term provides the initial diurnal and seasonal time dependence of the flux balance. The heating of the air-land and air ocean thermal reservoir interfaces produces the thermal gradients needed to dissipate the absorbed solar flux as heat. Evaporation also depends on the humidity gradient and the wind speed.

The total surface blackbody LWIR emission is given by Stefan's Law. The downward LWIR flux from the atmosphere should be calculated using radiative transfer theory. However, this may be simplified for discussion purposes by using Stefan's Law modified with a fixed atmospheric spectral window [IEEE, 1993]. The net LWIR flux then becomes:

$$\Delta Q_{\text{irnet}} = \sigma(\varepsilon T_s^4 - T_a^4) + \Delta Q_{\text{irwin}} \quad (\text{A6})$$

Here, σ is Stefan's constant, ε is the surface emissivity, T_s is the surface temperature, T_a is the surface air temperature and ΔQ_{irwin} is the LWIR transmission window loss. The spectral window can be set for example to 900 to 1100 cm^{-1} , which gives a window transmission flux of approximately 50 W m^{-2} at 288 K (15 C). Eqn. A6 provides a simple illustration of a complex LWIR flux balance process.

Convection is a complex turbulent mixing process. The convective surface cooling or sensible heat flux is often simplified by using a single convection coefficient k_{conv} and the bulk surface - air temperature difference.

$$\Delta Q_{\text{sens}} = k_{\text{conv}}(T_s - T_a) \quad (\text{A7})$$

Over dry land, k_{conv} is approximately 15 to 20 $\text{W m}^{-2} \text{K}^{-1}$ [Clark, 2011]. Over the oceans it is near 5 $\text{W m}^{-2} \text{K}^{-1}$ [Sahlee et al, 2008]. Here, the air temperature is taken as the MSAT temperature. Definitions may vary in the literature.

The surface is also cooled by water evaporation that is coupled to the convective flux. This reduces the surface temperature rise. Over water, the latent heat flux depends on the water surface humidity

gradient and the wind speed [Yu, 2007]. Over land, the description of the surface evaporation (evapotranspiration) is complex [Mengelkamp et al, 2006]. The latent heat flux usually peaks during the middle of the day and decreases significantly at night. However, the flux may also be limited by the transport of subsurface moisture to the surface. The ocean latent heat flux can be calculated using [Yu, 2007]:

$$\Delta Q_{\text{lat}} = k_{\text{lat}}(P_{T_{\text{ws}}} - R_h P_{T_{\text{wa}}})U \quad (\text{A8})$$

Here, k_{lat} is an empirical convection coefficient, $P_{T_{\text{ws}}}$ is the saturated water vapor concentration at the surface temperature T_s , $P_{T_{\text{wa}}}$ is the saturated water vapor concentration at the surface air temperature T_a , R_h is the relative humidity and U is the wind speed. Over the oceans, convection can continue at night because the cooler water produced at the surface sinks and is replaced by warmer water from the bulk ocean below.

Over land, the subsurface heat transfer process is conduction, which depends on the subsurface thermal gradient, the subsurface depth, x , and the thermal conductivity, k_{cnd} .

$$Q_{\text{ssc}} = k_{\text{cnd}}(T_s - T_{\text{ss}})/x \quad (\text{A9})$$

The thermal conductivity may be calculated analytically using a finite element approach [Billo, 2007]. Over the ocean, almost all of the solar flux is transmitted through the ocean surface. Ocean heating has to be calculated using a combination of depth dependent solar absorption from Eqn. A5 and downward layer mixing [Clark, 2013a, 2013b, 2011].

Eqns. A1 through A9 provide a basic description of the time dependent surface energy transfer. The full details of the fluid dynamics are complex, so the equations include several simplifications to the energy transfer processes. In particular, Eqn. A7 uses a bulk parametric description of the sensible heat convection and Eqn. A8 assumes linear relationship between wind speed and ocean surface evaporation. However, these equations provide a suitable framework that may be used to examine surface cooling and the ocean surface flux balance.

The incorporation of the surface flux balance equations into models of the land and ocean surface temperatures will now be considered.

A2: Land Surface Temperature Model

The model used to calculate the land surface temperature is illustrated schematically in Figure A1. The various flux terms were coupled into a surface layer 1 cm thick. The thermal properties of this layer were those of dry sand. The surface layer was also coupled into a subsurface thermal conduction model constructed following the finite element method described by Billo [2007]. 200 layers 1 cm thick were used in the model and the lowest layer was set to remain at a temperature of 10 C. The numerical values used are given in Table 1. The model time step was 1 minute. The calculation was run for a 1 year simulation (365x24x60 steps). The computer run time was

approximately 30 seconds. The data were output at 2 hour intervals. In addition, the full 1 minute step data sets were output for the solstice and equinox points for days 81, 172, 264 and 355. As discussed below, the heat capacity of the land subsurface reservoir was not large enough to simulate the observed diurnal and seasonal phase shifts. Additional air heating and cooling terms were added to provide the correct diurnal phase shift. An offset was incorporated into the transition temperature algorithm to simulate the seasonal phase shift.

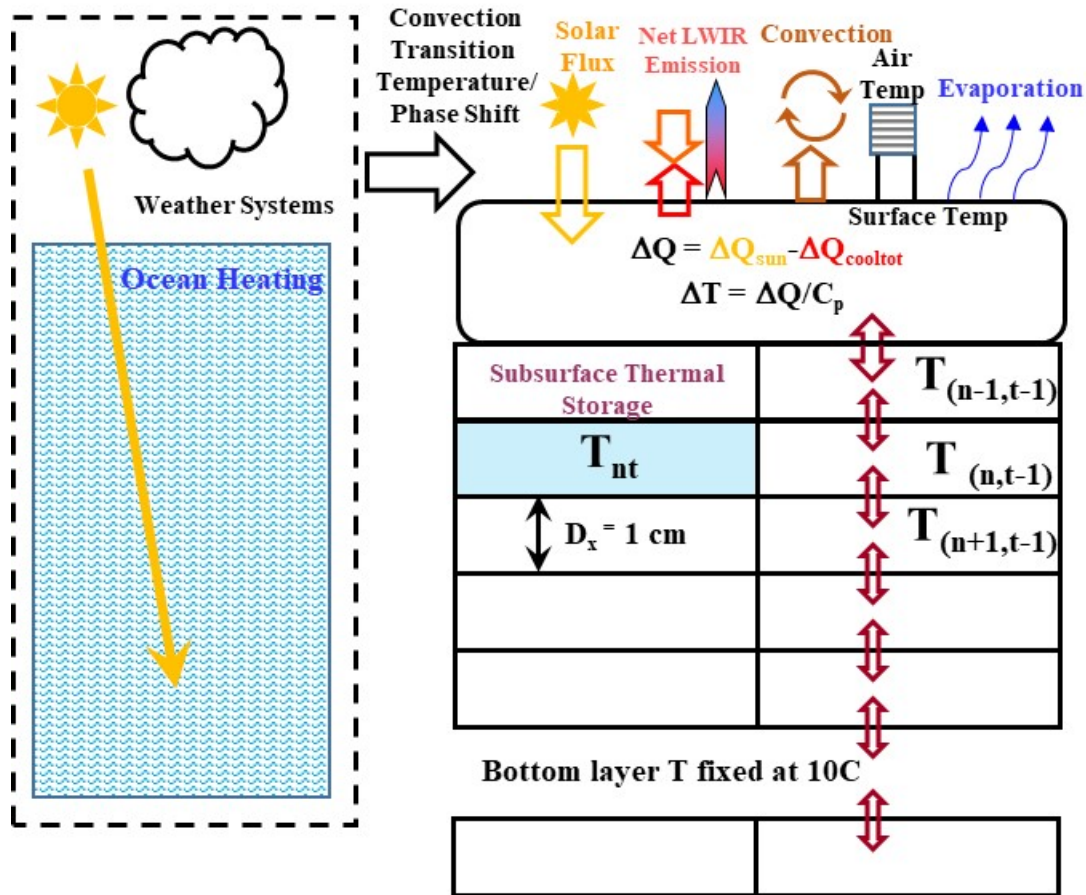


Figure A1: Land surface temperature model structure (schematic)

Table A1: Numerical Values Used in the Thermal Conduction Model

Sand		
Density [r]	1.68E+03	kg.m-3
Heat Capacity [Cp]	8.16E-01	kJ.kg-1.C-1
Thermal Conductivity	3.35E-04	kJ.m-1.s-1.C-1
e=k/Cp.r	2.44E-07	s-1 m2
dt	6.00E+01	sec
dx	1.00E-02	m
f = e.dt/dx^2	0.147	const

The various flux terms were calculated as follows:

Solar Flux: This was calculated from Eqns. A2, A3 and A4 using the day of year, time of day, latitude and declination as inputs. The day numbers were offset to place the minimum solar flux at the winter solstice, day 355.

The absorption term was set to 0.885. The change in surface reflectivity was simulated by including the Fresnel reflection for $n=1.5$ at the solar angle of incidence.

A coupling fraction coefficient was also added to the solar flux. This could be set from 1 to 0 to simulate reductions in solar flux for example from cloud cover.

Transition Temperature: This was calculated using a daily transition temperature T_{trans} given by

$$T_{\text{trans}} = T_{\text{transmax}} * \text{Cos}^3\theta + T_{\text{offset}} \quad (\text{A10})$$

Where T_{transmax} is an empirical maximum temperature set in the model and θ is the daily solar zenith angle at noon. An empirical minimum offset temperature (T_{offset}) is also set in the model. These were adjusted to provide an approximate match to the daily minimum MSAT profile for the weather station data of interest.

The form of Eqn. 10 was derived from an approximate fit to the latitude band average ocean air temperatures published by Yu et al [2008]. The three cosine terms multiplied together follow from 1) Lambert's cosine law, 2) the approximate change in atmospheric optical transmission with latitude and 3) the approximate change in surface reflectivity with angle. The data are shown in Figure A2.

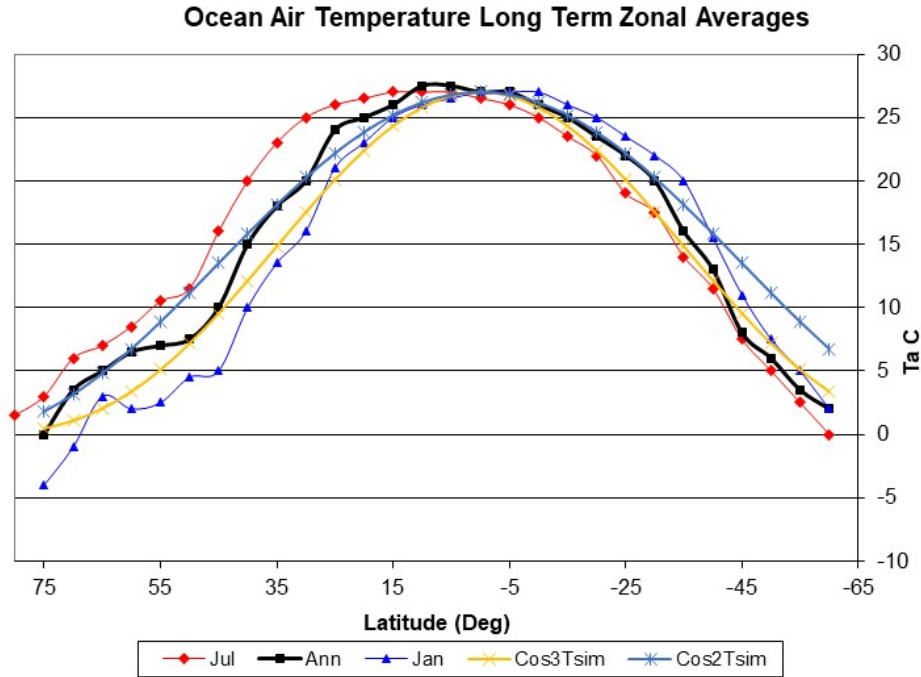


Figure A2: Latitude average ocean air temperatures and \cos^2 and \cos^3 fit terms

Air Temperature: The air temperature T_a was initially calculated using:

$$T_a = T_{\text{transition}} + f_{\text{tr}}*(T_{\text{surf}} - T_{\text{transition}}) \quad (\text{A11})$$

Where f_{tr} is a fraction empirically set in the model. This was set to 0.5.

In order to simulate the diurnal phase shift, the air temperature algorithm was modified to include a heating and a cooling term. The heating term was set as a fraction of the surface convection and the cooling term was set as a fraction of the difference between the air temperature and the transition temperature. The values used were 1/2000 for the heating and 1/40 for the cooling.

The air temperature was reset at the start of each day using Eq. A11. It was then calculated using:

$$T_a = T_a + T_{\text{conv}}/2000 - (T_a - T_{\text{trans}})/40 \quad (\text{A12})$$

This approach gave reasonable values for the air temperature and the diurnal phase shift.

Atmospheric LWIR Transmission Window Flux: The LWIR transmission flux was calculated using Eqn. A6. The transmission window flux was set to 40 W m^{-2} . The surface emissivity was set to 0.95.

Convection and Latent Heat Fluxes: The convection or sensible heat flux was calculated using Eqn. A7. The convection constant was set to 25 W C^{-1} . The latent heat was set as a fraction of the solar flux. The model was initially run using dry sand with the latent heat fraction set to zero.

Model Run Configuration: The following inputs were adjusted to simulate the weather station data.

Latitude, transition temperature range and offset, seasonal phase shift and solar intensity coefficient.

The surface absorption, surface emissivity, convection constant, air temperature phase heating and cooling constants and layer thickness were generally kept constant.

The model was run until the output value of the surface temperature at the end of day 365 matched the input value at the start of day 1. The output values at the end of day 365 were copied to the input values at the start of day 1 after each run. Usually only 1 iteration was required for the temperature values to stabilize.

Additional post processing macros and worksheet templates were used to generate the 365 day max/min MSAT data for comparison to the weather station data and to generate summary plots.

A3: Ocean Surface Temperature Model

The ocean surface temperature model is illustrated schematically in Figure A3. 110 x 1 m ocean layers were used. The surface flux terms were coupled into the first layer. The absorbed solar flux in each layer was calculated using Eq. A5. The values were determined by combining the solar spectral distribution from ASTM G173 with the water absorption values from Hale and Querry [1972]. Both data sets were converted to a spectral resolution of 5 nm and used to calculate the total absorption fraction for each layer. A scattering coefficient of 0.0007 m^{-1} was also included to account for ocean water scattering. The values used are plotted in Figure A4. The time step used was 0.5 hours and the full 17520 x 110 data set was output into a worksheet.

Solar Flux: This was calculated from Eqns. A2, A3 and A4 using the day of year, time of day, latitude and declination as inputs. The day numbers were offset to place the minimum solar flux at the winter solstice, day 355.

The change in surface reflectivity was simulated by including the Fresnel reflection for $n=1.3$ at the solar angle of incidence.

A coupling fraction coefficient was also added to the solar flux term. This could be set from 1 to 0 to simulate reductions in solar flux for example from cloud cover.

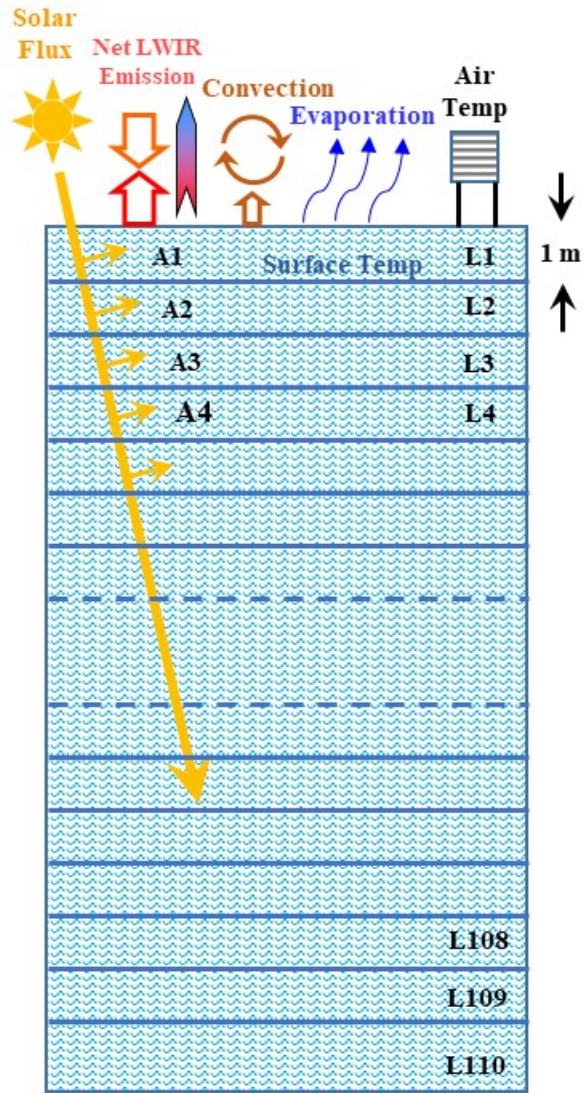


Figure A3: Ocean surface temperature model (schematic)

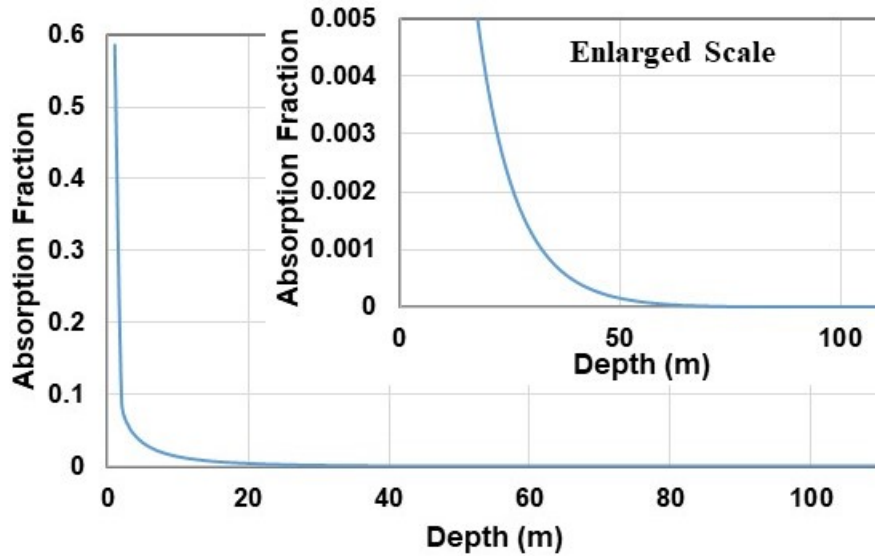


Figure A4: Absorption coefficient inputs for Eq. A5 for ocean solar absorption.

Air Temperature: The air temperature T_a was set to be 1 C below the ocean (layer 1) surface temperature.

Atmospheric LWIR Transmission Window Flux: The LWIR transmission flux was calculated using Eqn. A6. The transmission window flux was set to 45 W m^{-2} . The surface emissivity was set to 0.95.

Convection Flux: The convection or sensible heat flux was calculated using Eqn. A7. The convection constant was set to 5 W K^{-1} .

Latent Heat Flux: The latent heat flux was calculated using Eqn. A8. The relative humidity was set to 70%. The water vapor pressure was calculated using a 6th order polynomial fit to published water vapor pressure – temperature data. The coefficients were:

$$\begin{aligned} \text{VP} = & 6.87431\text{E}11 * T^6 + 1.71479\text{E}08 * T^5 + 2.1863\text{E}06 * T^4 + 0.000190906 * T^3 + 0.01083577 * T^2 \\ & + 0.3407838 * T + 4.476147 \text{ (mm Hg)} \end{aligned} \quad (\text{Eq. A13})$$

The coupling coefficient k_{lat} was adjusted in the model until the surface temperature at the end of day 365 matched the input surface temperature at the start of day 1. Usually the agreement was better than 0.01 C.

Values for the wind speed were taken from Yu et al [2007]. To account for the summer decrease in wind speed, a maximum winter wind speed and a value for the summer decrease were input into the model. The wind speed was decreased using a sine function based on the day value with a maximum decrease at midyear.

It is also important to note that the rate of evaporation also increases faster with temperature than the LWIR blackbody emission. Figure A5 shows the increase in LWIR exchange energy and evaporative cooling flux calculated from Eqn. 8 vs. ocean surface temperature. For the evaporation, the RH was 80% and the surface temperature difference was 1 C.

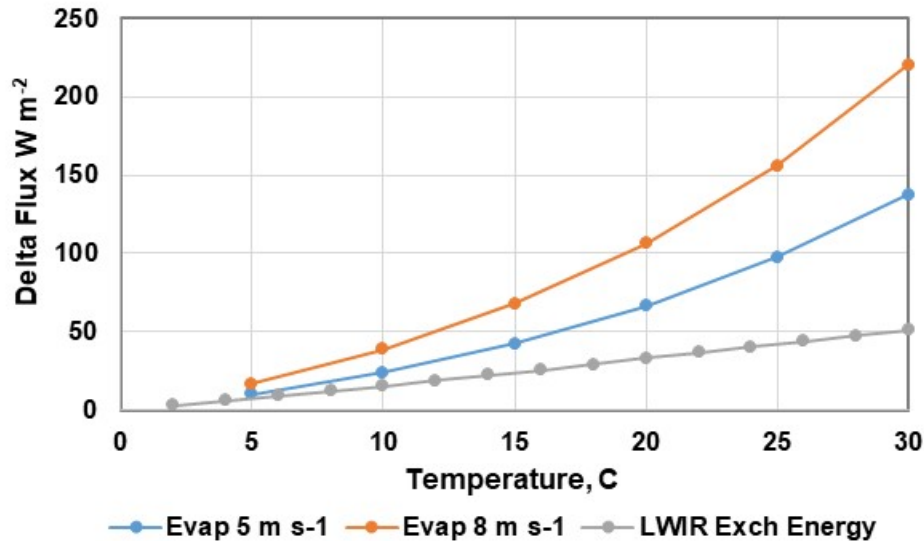


Figure A5: Increase in ocean surface cooling flux vs. surface temperature

Ocean Layer Mixing

Ocean mixing is a complex Rayleigh-Benard convection process with additional lateral transport. A relatively simple mixing scheme was used that simulated the seasonal temperature variation and provided reasonable phase shift results. However, the summer stratification extended closer to the surface than in the Argo float data. The primary interest here is to demonstrate the seasonal phase shift for realistic ocean surface temperatures and wind speeds, so no attempt was made to match the stratification to Argo data.

The ocean layers were mixed at the end of each 0.5 hour time step iteration. A 10 layer exponential diffusion mixing was first used to blend the layers. The layers were then mixed using a simple layer temperature algorithm. The cooler surface layers were mixed downward sequentially until the uniform mixed layer matched the temperature of the layer below. Since most of the solar flux was absorbed in the first layer, additional mixing of this layer was simulated by adjusting the solar absorption coefficients. This was needed to reduce the summer surface temperature rise, especially at higher latitudes. A fraction of the flux absorbed was removed from the first layer and distributed over the next 100 layers. This is illustrated in Figure A6. In this case, half of the absorbed solar flux from layer 1 is removed and distributed over the next 100 layers. The value of the removed flux is divided by 100. 2 units are added to layer 2, decreasing to 1 unit at layer 51 and zero at layer 101.

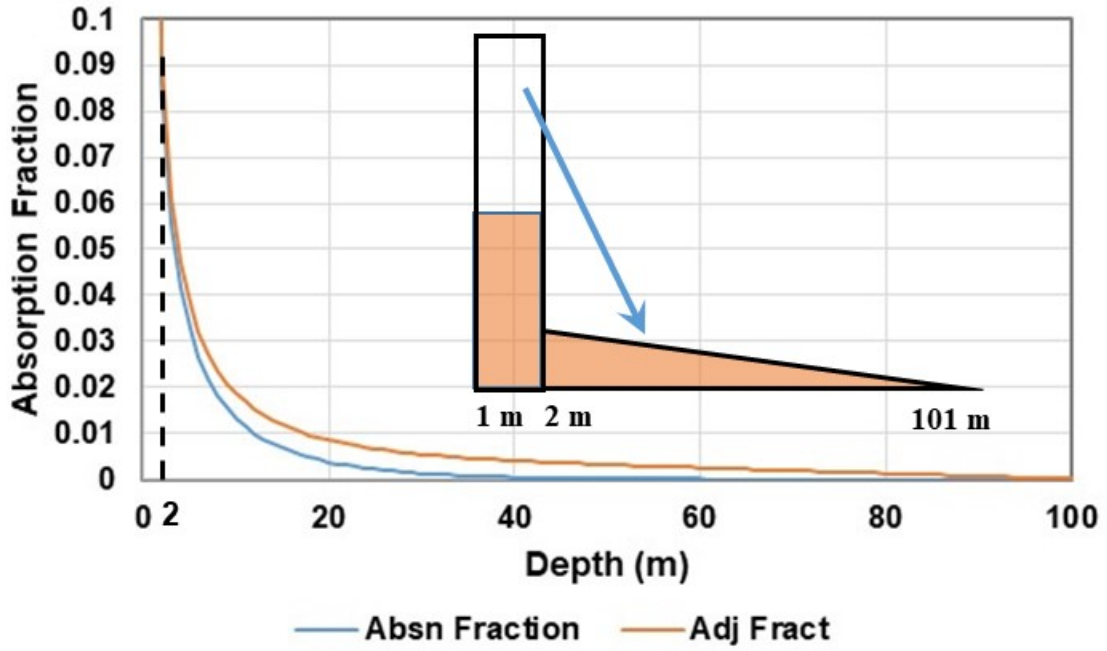


Figure A6: Absorbed flux mixing. A fraction of the flux absorbed in the first layer is removed and distributed over the layers below.